

Study of the decay $D_s^+ \rightarrow K^+ K^- e^+ \nu_e$

B. Aubert,¹ M. Bona,¹ Y. Karyotakis,¹ J. P. Lees,¹ V. Poireau,¹ E. Prencipe,¹ X. Prudent,¹ V. Tisserand,¹ J. Garra Tico,² E. Grauges,² L. Lopez,^{3,4} A. Palano,^{3,4} M. Pappagallo,^{3,4} G. Eigen,⁵ B. Stugu,⁵ L. Sun,⁵ G. S. Abrams,⁶ M. Battaglia,⁶ D. N. Brown,⁶ R. N. Cahn,⁶ R. G. Jacobsen,⁶ L. T. Kerth,⁶ Yu. G. Kolomensky,⁶ G. Kukartsev,⁶ G. Lynch,⁶ I. L. Osipenkov,⁶ M. T. Ronan,^{6,*} K. Tackmann,⁶ T. Tanabe,⁶ C. M. Hawkes,⁷ N. Soni,⁷ A. T. Watson,⁷ H. Koch,⁸ T. Schroeder,⁸ D. Walker,⁹ D. J. Asgeirsson,¹⁰ T. Cuhadar-Donszelmann,¹⁰ B. G. Fulsom,¹⁰ C. Hearty,¹⁰ T. S. Mattison,¹⁰ J. A. McKenna,¹⁰ M. Barrett,¹¹ A. Khan,¹¹ L. Teodorescu,¹¹ V. E. Blinov,¹² A. D. Bukin,¹² A. R. Buzykaev,¹² V. P. Druzhinin,¹² V. B. Golubev,¹² A. P. Onuchin,¹² S. I. Serednyakov,¹² Yu. I. Skovpen,¹² E. P. Solodov,¹² K. Yu. Todyshev,¹² M. Bondioli,¹³ S. Curry,¹³ I. Eschrich,¹³ D. Kirkby,¹³ A. J. Lankford,¹³ P. Lund,¹³ M. Mandelkern,¹³ E. C. Martin,¹³ D. P. Stoker,¹³ S. Abachi,¹⁴ C. Buchanan,¹⁴ J. W. Gary,¹⁵ F. Liu,¹⁵ O. Long,¹⁵ B. C. Shen,^{15,*} G. M. Vitug,¹⁵ Z. Yasin,¹⁵ L. Zhang,¹⁵ V. Sharma,¹⁶ C. Campagnari,¹⁷ T. M. Hong,¹⁷ D. Kovalskiy,¹⁷ M. A. Mazur,¹⁷ J. D. Richman,¹⁷ T. W. Beck,¹⁸ A. M. Eisner,¹⁸ C. J. Flacco,¹⁸ C. A. Heusch,¹⁸ J. Kroseberg,¹⁸ W. S. Lockman,¹⁸ T. Schalk,¹⁸ B. A. Schumm,¹⁸ A. Seiden,¹⁸ L. Wang,¹⁸ M. G. Wilson,¹⁸ L. O. Winstrom,¹⁸ C. H. Cheng,¹⁹ D. A. Doll,¹⁹ B. Echenard,¹⁹ F. Fang,¹⁹ D. G. Hitlin,¹⁹ I. Narsky,¹⁹ T. Piatenko,¹⁹ F. C. Porter,¹⁹ R. Andreassen,²⁰ G. Mancinelli,²⁰ B. T. Meadows,²⁰ K. Mishra,²⁰ M. D. Sokoloff,²⁰ F. Blanc,²¹ P. C. Bloom,²¹ W. T. Ford,²¹ A. Gaz,²¹ J. F. Hirschauer,²¹ A. Kreisel,²¹ M. Nagel,²¹ U. Nauenberg,²¹ J. G. Smith,²¹ K. A. Ulmer,²¹ S. R. Wagner,²¹ R. Ayad,^{22,+} A. Soffer,^{22,‡} W. H. Toki,²² R. J. Wilson,²² D. D. Altenburg,²³ E. Feltresi,²³ A. Hauke,²³ H. Jasper,²³ M. Karbach,²³ J. Merkel,²³ A. Petzold,²³ B. Spaan,²³ K. Wacker,²³ M. J. Kobel,²⁴ W. F. Mader,²⁴ R. Nogowski,²⁴ K. R. Schubert,²⁴ R. Schwierz,²⁴ J. E. Sundermann,²⁴ A. Volk,²⁴ D. Bernard,²⁵ G. R. Bonneaud,²⁵ E. Latour,²⁵ Ch. Thiebaut,²⁵ M. Verderi,²⁵ P. J. Clark,²⁶ W. Gradl,²⁶ S. Playfer,²⁶ J. E. Watson,²⁶ M. Andreotti,^{27,28} D. Bettoni,²⁷ C. Bozzi,²⁷ R. Calabrese,^{27,28} A. Cecchi,^{27,28} G. Cibinetto,^{27,28} P. Franchini,^{27,28} E. Luppi,^{27,28} M. Negrini,^{27,28} A. Petrella,^{27,28} L. Piemontese,²⁷ V. Santoro,^{27,28} R. Baldini-Ferroli,²⁹ A. Calcaterra,²⁹ R. de Sangro,²⁹ G. Finocchiaro,²⁹ S. Pacetti,²⁹ P. Patteri,²⁹ I. M. Peruzzi,^{29,§} M. Piccolo,²⁹ M. Rama,²⁹ A. Zallo,²⁹ A. Buzzo,³⁰ R. Contri,^{30,31} M. Lo Vetere,^{30,31} M. M. Macri,³⁰ M. R. Monge,^{30,31} S. Passaggio,³⁰ C. Patrignani,^{30,31} E. Robutti,³⁰ A. Santroni,^{30,31} S. Tosi,^{30,31} K. S. Chaisanguanthum,³² M. Morii,³² R. S. Dubitzky,³³ J. Marks,³³ S. Schenk,³³ U. Uwer,³³ V. Klose,³⁴ H. M. Lacker,³⁴ G. De Nardo,^{35,36} L. Lista,³⁵ D. Monorchio,^{35,36} G. Onorato,^{35,36} C. Sciacca,^{35,36} D. J. Bard,³⁷ P. D. Dauncey,³⁷ J. A. Nash,³⁷ W. Panduro Vazquez,³⁷ M. Tibbetts,³⁷ P. K. Behera,³⁸ X. Chai,³⁸ M. J. Charles,³⁸ U. Mallik,³⁸ J. Cochran,³⁹ H. B. Crawley,³⁹ L. Dong,³⁹ W. T. Meyer,³⁹ S. Prell,³⁹ E. I. Rosenberg,³⁹ A. E. Rubin,³⁹ Y. Y. Gao,⁴⁰ A. V. Gritsan,⁴⁰ Z. J. Guo,⁴⁰ C. K. Lae,⁴⁰ A. G. Denig,⁴¹ M. Fritsch,⁴¹ G. Schott,⁴¹ N. Arnaud,⁴² J. Béquilleux,⁴² A. D'Orazio,⁴² M. Davier,⁴² J. Firmino da Costa,⁴² G. Grosdidier,⁴² A. Höcker,⁴² V. Lepeltier,⁴² F. Le Diberder,⁴² A. M. Lutz,⁴² S. Pruvot,⁴² P. Roudeau,⁴² M. H. Schune,⁴² J. Serrano,⁴² V. Sordini,^{42,||} A. Stocchi,⁴² G. Wormser,⁴² D. J. Lange,⁴³ D. M. Wright,⁴³ I. Bingham,⁴⁴ J. P. Burke,⁴⁴ C. A. Chavez,⁴⁴ J. R. Fry,⁴⁴ E. Gabathuler,⁴⁴ R. Gamet,⁴⁴ D. E. Hutchcroft,⁴⁴ D. J. Payne,⁴⁴ C. Touramanis,⁴⁴ A. J. Bevan,⁴⁵ K. A. George,⁴⁵ F. Di Lodovico,⁴⁵ R. Sacco,⁴⁵ M. Sigamani,⁴⁵ G. Cowan,⁴⁶ H. U. Flaecher,⁴⁶ D. A. Hopkins,⁴⁶ S. Paramesvaran,⁴⁶ F. Salvatore,⁴⁶ A. C. Wren,⁴⁶ D. N. Brown,⁴⁷ C. L. Davis,⁴⁷ K. E. Alwyn,⁴⁸ N. R. Barlow,⁴⁸ R. J. Barlow,⁴⁸ Y. M. Chia,⁴⁸ C. L. Edgar,⁴⁸ G. D. Lafferty,⁴⁸ T. J. West,⁴⁸ J. I. Yi,⁴⁸ J. Anderson,⁴⁹ C. Chen,⁴⁹ A. Jawahery,⁴⁹ D. A. Roberts,⁴⁹ G. Simi,⁴⁹ J. M. Tuggle,⁴⁹ C. Dallapiccola,⁵⁰ S. S. Hertzbach,⁵⁰ X. Li,⁵⁰ E. Salvati,⁵⁰ S. Saremi,⁵⁰ R. Cowan,⁵¹ D. Dujmic,⁵¹ P. H. Fisher,⁵¹ K. Koeneke,⁵¹ G. Sciolla,⁵¹ M. Spitznagel,⁵¹ F. Taylor,⁵¹ R. K. Yamamoto,⁵¹ M. Zhao,⁵¹ S. E. Mclachlin,^{52,*} P. M. Patel,⁵² S. H. Robertson,⁵² A. Lazzaro,^{53,54} V. Lombardo,⁵³ F. Palombo,^{53,54} J. M. Bauer,⁵⁵ L. Cremaldi,⁵⁵ V. Eschenburg,⁵⁵ R. Godang,^{55,||} R. Kroeger,⁵⁵ D. A. Sanders,⁵⁵ D. J. Summers,⁵⁵ H. W. Zhao,⁵⁵ M. Simard,⁵⁶ P. Taras,⁵⁶ F. B. Viaud,⁵⁶ H. Nicholson,⁵⁷ M. A. Baak,⁵⁸ G. Raven,⁵⁸ H. L. Snoek,⁵⁸ C. P. Jessop,⁵⁹ K. J. Knoepfel,⁵⁹ J. M. LoSecco,⁵⁹ W. F. Wang,⁵⁹ G. Benelli,⁶⁰ L. A. Corwin,⁶⁰ K. Honscheid,⁶⁰ H. Kagan,⁶⁰ R. Kass,⁶⁰ J. P. Morris,⁶⁰ A. M. Rahimi,⁶⁰ J. J. Regensburger,⁶⁰ S. J. Sekula,⁶⁰ Q. K. Wong,⁶⁰ N. L. Blount,⁶¹ J. Brau,⁶¹ R. Frey,⁶¹ O. Igonkina,⁶¹ J. A. Kolb,⁶¹ M. Lu,⁶¹ R. Rahmat,⁶¹ N. B. Sinev,⁶¹ D. Strom,⁶¹ J. Strube,⁶¹ E. Torrence,⁶¹ G. Castelli,^{62,63} N. Gagliardi,^{62,63} M. Margoni,^{62,63} M. Morandin,⁶² M. Posocco,⁶² M. Rotondo,⁶² F. Simonetto,^{62,63} R. Stroili,^{62,63} C. Voci,^{62,63} P. del Amo Sanchez,⁶⁴ E. Ben-Haim,⁶⁴ H. Briand,⁶⁴ G. Calderini,⁶⁴ J. Chauveau,⁶⁴ P. David,⁶⁴ L. Del Buono,⁶⁴ O. Hamon,⁶⁴ Ph. Leruste,⁶⁴ J. Ocariz,⁶⁴ A. Perez,⁶⁴ J. Prendki,⁶⁴ L. Gladney,⁶⁵ M. Biasini,^{66,67} R. Covarelli,^{66,67} E. Manoni,^{66,67} C. Angelini,^{68,69} G. Batignani,^{68,69} S. Bettarini,^{68,69} M. Carpinelli,^{68,69,**} A. Cervelli,^{68,69} F. Forti,^{68,69} M. A. Giorgi,^{68,69} A. Lusiani,^{68,70} G. Marchiori,^{68,69} M. Morganti,^{68,69} N. Neri,^{68,69} E. Paoloni,^{68,69} G. Rizzo,^{68,69} J. J. Walsh,⁶⁸ J. Biesiada,⁷¹ D. Lopes Pegna,⁷¹ C. Lu,⁷¹ J. Olsen,⁷¹ A. J. S. Smith,⁷¹ A. V. Telnov,⁷¹ F. Anulli,⁷² E. Baracchini,^{72,73} G. Cavoto,⁷² D. del Re,^{72,73} E. Di Marco,^{72,73} R. Faccini,^{72,73} F. Ferrarotto,⁷² F. Ferroni,^{72,73} M. Gaspero,^{72,73} P. D. Jackson,⁷²

L. Li Gioi,⁷² M. A. Mazzoni,⁷² S. Morganti,⁷² G. Piredda,⁷² F. Polci,^{72,73} F. Renga,^{72,73} C. Voena,⁷² M. Ebert,⁷⁴ T. Hartmann,⁷⁴ H. Schröder,⁷⁴ R. Waldi,⁷⁴ T. Adye,⁷⁵ B. Franek,⁷⁵ E. O. Olaiya,⁷⁵ W. Roethel,⁷⁵ F. F. Wilson,⁷⁵ S. Emery,⁷⁶ M. Escalier,⁷⁶ L. Esteve,⁷⁶ A. Gaidot,⁷⁶ S. F. Ganzhur,⁷⁶ G. Hamel de Monchenault,⁷⁶ W. Kozanecki,⁷⁶ G. Vasseur,⁷⁶ Ch. Yèche,⁷⁶ M. Zito,⁷⁶ X. R. Chen,⁷⁷ H. Liu,⁷⁷ W. Park,⁷⁷ M. V. Purohit,⁷⁷ R. M. White,⁷⁷ J. R. Wilson,⁷⁷ M. T. Allen,⁷⁸ D. Aston,⁷⁸ R. Bartoldus,⁷⁸ P. Bechtel,⁷⁸ J. F. Benitez,⁷⁸ R. Cenci,⁷⁸ J. P. Coleman,⁷⁸ M. R. Convery,⁷⁸ J. C. Dingfelder,⁷⁸ J. Dorfan,⁷⁸ G. P. Dubois-Felsmann,⁷⁸ W. Dunwoodie,⁷⁸ R. C. Field,⁷⁸ A. M. Gabareen,⁷⁸ S. J. Gowdy,⁷⁸ M. T. Graham,⁷⁸ P. Grenier,⁷⁸ C. Hast,⁷⁸ W. R. Innes,⁷⁸ J. Kaminski,⁷⁸ M. H. Kelsey,⁷⁸ H. Kim,⁷⁸ P. Kim,⁷⁸ M. L. Kocian,⁷⁸ D. W. G. S. Leith,⁷⁸ S. Li,⁷⁸ B. Lindquist,⁷⁸ S. Luitz,⁷⁸ V. Luth,⁷⁸ H. L. Lynch,⁷⁸ D. B. MacFarlane,⁷⁸ H. Marsiske,⁷⁸ R. Messner,⁷⁸ D. R. Muller,⁷⁸ H. Neal,⁷⁸ S. Nelson,⁷⁸ C. P. O'Grady,⁷⁸ I. Ofte,⁷⁸ A. Perazzo,⁷⁸ M. Perl,⁷⁸ B. N. Ratcliff,⁷⁸ A. Roodman,⁷⁸ A. A. Salnikov,⁷⁸ R. H. Schindler,⁷⁸ J. Schwiening,⁷⁸ A. Snyder,⁷⁸ D. Su,⁷⁸ M. K. Sullivan,⁷⁸ K. Suzuki,⁷⁸ S. K. Swain,⁷⁸ J. M. Thompson,⁷⁸ J. Va'vra,⁷⁸ A. P. Wagner,⁷⁸ M. Weaver,⁷⁸ C. A. West,⁷⁸ W. J. Wisniewski,⁷⁸ M. Wittgen,⁷⁸ D. H. Wright,⁷⁸ H. W. Wulsin,⁷⁸ A. K. Yarritu,⁷⁸ K. Yi,⁷⁸ C. C. Young,⁷⁸ V. Ziegler,⁷⁸ P. R. Burchat,⁷⁹ A. J. Edwards,⁷⁹ S. A. Majewski,⁷⁹ T. S. Miyashita,⁷⁹ B. A. Petersen,⁷⁹ L. Wilden,⁷⁹ S. Ahmed,⁸⁰ M. S. Alam,⁸⁰ R. Bula,⁸⁰ J. A. Ernst,⁸⁰ B. Pan,⁸⁰ M. A. Saeed,⁸⁰ S. B. Zain,⁸⁰ S. M. Spanier,⁸¹ B. J. Wogslund,⁸¹ R. Eckmann,⁸² J. L. Ritchie,⁸² A. M. Ruland,⁸² C. J. Schilling,⁸² R. F. Schwitters,⁸² B. W. Drummond,⁸³ J. M. Izen,⁸³ X. C. Lou,⁸³ F. Bianchi,^{84,85} D. Gamba,^{84,85} M. Pelliccioni,^{84,85} M. Bomben,^{86,87} L. Bosisio,^{86,87} C. Cartaro,^{86,87} G. Della Ricca,^{86,87} L. Lanceri,^{86,87} L. Vitale,^{86,87} V. Azzolini,⁸⁸ N. Lopez-March,⁸⁸ F. Martinez-Vidal,⁸⁸ D. A. Milanes,⁸⁸ A. Oyangueren,⁸⁸ J. Albert,⁸⁹ Sw. Banerjee,⁸⁹ B. Bhuyan,⁸⁹ H. H. F. Choi,⁸⁹ K. Hamano,⁸⁹ R. Kowalewski,⁸⁹ M. J. Lewczuk,⁸⁹ I. M. Nugent,⁸⁹ J. M. Roney,⁸⁹ R. J. Sobie,⁸⁹ T. J. Gershon,⁹⁰ P. F. Harrison,⁹⁰ J. Ilic,⁹⁰ T. E. Latham,⁹⁰ G. B. Mohanty,⁹⁰ H. R. Band,⁹¹ X. Chen,⁹¹ S. Dasu,⁹¹ K. T. Flood,⁹¹ Y. Pan,⁹¹ M. Pierini,⁹¹ R. Prepost,⁹¹ C. O. Vuosalo,⁹¹ and S. L. Wu⁹¹

(BABAR Collaboration)

¹Laboratoire de Physique des Particules, IN2P3/CNRS et Université de Savoie, F-74941 Annecy-Le-Vieux, France

²Universitat de Barcelona, Facultat de Fisica, Departament ECM, E-08028 Barcelona, Spain

³INFN Sezione di Bari, I-70126 Bari, Italy

⁴Dipartimento di Fisica, Università di Bari, I-70126 Bari, Italy

⁵University of Bergen, Institute of Physics, N-5007 Bergen, Norway

⁶Lawrence Berkeley National Laboratory and University of California, Berkeley, California 94720, USA

⁷University of Birmingham, Birmingham, B15 2TT, United Kingdom

⁸Ruhr Universität Bochum, Institut für Experimentalphysik I, D-44780 Bochum, Germany

⁹University of Bristol, Bristol BS8 1TL, United Kingdom

¹⁰University of British Columbia, Vancouver, British Columbia, Canada V6T 1Z1

¹¹Brunel University, Uxbridge, Middlesex UB8 3PH, United Kingdom

¹²Budker Institute of Nuclear Physics, Novosibirsk 630090, Russia

¹³University of California at Irvine, Irvine, California 92697, USA

¹⁴University of California at Los Angeles, Los Angeles, California 90024, USA

¹⁵University of California at Riverside, Riverside, California 92521, USA

¹⁶University of California at San Diego, La Jolla, California 92093, USA

¹⁷University of California at Santa Barbara, Santa Barbara, California 93106, USA

¹⁸University of California at Santa Cruz, Institute for Particle Physics, Santa Cruz, California 95064, USA

¹⁹California Institute of Technology, Pasadena, California 91125, USA

²⁰University of Cincinnati, Cincinnati, Ohio 45221, USA

²¹University of Colorado, Boulder, Colorado 80309, USA

²²Colorado State University, Fort Collins, Colorado 80523, USA

²³Technische Universität Dortmund, Fakultät Physik, D-44221 Dortmund, Germany

²⁴Technische Universität Dresden, Institut für Kern- und Teilchenphysik, D-01062 Dresden, Germany

²⁵Laboratoire Leprince-Ringuet, CNRS/IN2P3, Ecole Polytechnique, F-91128 Palaiseau, France

²⁶University of Edinburgh, Edinburgh EH9 3JZ, United Kingdom

²⁷INFN Sezione di Ferrara, I-44100 Ferrara, Italy

²⁸Dipartimento di Fisica, Università di Ferrara, I-44100 Ferrara, Italy

²⁹INFN Laboratori Nazionali di Frascati, I-00044 Frascati, Italy

³⁰INFN Sezione di Genova, I-16146 Genova, Italy

³¹Dipartimento di Fisica, Università di Genova, I-16146 Genova, Italy

³²Harvard University, Cambridge, Massachusetts 02138, USA

³³Universität Heidelberg, Physikalisches Institut, Philosophenweg 12, D-69120 Heidelberg, Germany

³⁴Humboldt-Universität zu Berlin, Institut für Physik, Newtonstr. 15, D-12489 Berlin, Germany

- ³⁵INFN Sezione di Napoli, I-80126 Napoli, Italy
- ³⁶Dipartimento di Scienze Fisiche, Università di Napoli Federico II, I-80126 Napoli, Italy
- ³⁷Imperial College London, London, SW7 2AZ, United Kingdom
- ³⁸University of Iowa, Iowa City, Iowa 52242, USA
- ³⁹Iowa State University, Ames, Iowa 50011-3160, USA
- ⁴⁰Johns Hopkins University, Baltimore, Maryland 21218, USA
- ⁴¹Universität Karlsruhe, Institut für Experimentelle Kernphysik, D-76021 Karlsruhe, Germany
- ⁴²Laboratoire de l'Accélérateur Linéaire, IN2P3/CNRS et Université Paris-Sud 11, Centre Scientifique d'Orsay, B. P. 34, F-91898 ORSAY Cedex, France
- ⁴³Lawrence Livermore National Laboratory, Livermore, California 94550, USA
- ⁴⁴University of Liverpool, Liverpool L69 7ZE, United Kingdom
- ⁴⁵Queen Mary, University of London, E1 4NS, United Kingdom
- ⁴⁶University of London, Royal Holloway and Bedford New College, Egham, Surrey TW20 0EX, United Kingdom
- ⁴⁷University of Louisville, Louisville, Kentucky 40292, USA
- ⁴⁸University of Manchester, Manchester M13 9PL, United Kingdom
- ⁴⁹University of Maryland, College Park, Maryland 20742, USA
- ⁵⁰University of Massachusetts, Amherst, Massachusetts 01003, USA
- ⁵¹Massachusetts Institute of Technology, Laboratory for Nuclear Science, Cambridge, Massachusetts 02139, USA
- ⁵²McGill University, Montréal, Québec, Canada H3A 2T8
- ⁵³INFN Sezione di Milano, I-20133 Milano, Italy
- ⁵⁴Dipartimento di Fisica, Università di Milano, I-20133 Milano, Italy
- ⁵⁵University of Mississippi, University, Mississippi 38677, USA
- ⁵⁶Université de Montréal, Physique des Particules, Montréal, Québec, Canada H3C 3J7
- ⁵⁷Mount Holyoke College, South Hadley, Massachusetts 01075, USA
- ⁵⁸NIKHEF, National Institute for Nuclear Physics and High Energy Physics, NL-1009 DB Amsterdam, The Netherlands
- ⁵⁹University of Notre Dame, Notre Dame, Indiana 46556, USA
- ⁶⁰Ohio State University, Columbus, Ohio 43210, USA
- ⁶¹University of Oregon, Eugene, Oregon 97403, USA
- ⁶²INFN Sezione di Padova, I-35131 Padova, Italy
- ⁶³Dipartimento di Fisica, Università di Padova, I-35131 Padova, Italy
- ⁶⁴Laboratoire de Physique Nucléaire et de Hautes Energies, IN2P3/CNRS, Université Pierre et Marie Curie-Paris6, Université Denis Diderot-Paris7, F-75252 Paris, France
- ⁶⁵University of Pennsylvania, Philadelphia, Pennsylvania 19104, USA
- ⁶⁶INFN Sezione di Perugia, I-06100 Perugia, Italy
- ⁶⁷Dipartimento di Fisica, Università di Perugia, I-06100 Perugia, Italy
- ⁶⁸INFN Sezione di Pisa, I-56127 Pisa, Italy
- ⁶⁹Dipartimento di Fisica, Università di Pisa, I-56127 Pisa, Italy
- ⁷⁰Scuola Normale Superiore di Pisa, I-56127 Pisa, Italy
- ⁷¹Princeton University, Princeton, New Jersey 08544, USA
- ⁷²INFN Sezione di Roma, I-00185 Roma, Italy
- ⁷³Dipartimento di Fisica, Università di Roma La Sapienza, I-00185 Roma, Italy
- ⁷⁴Universität Rostock, D-18051 Rostock, Germany
- ⁷⁵Rutherford Appleton Laboratory, Chilton, Didcot, Oxon, OX11 0QX, United Kingdom
- ⁷⁶DSM/Dapnia, CEA/Saclay, F-91191 Gif-sur-Yvette, France
- ⁷⁷University of South Carolina, Columbia, South Carolina 29208, USA
- ⁷⁸Stanford Linear Accelerator Center, Stanford, California 94309, USA
- ⁷⁹Stanford University, Stanford, California 94305-4060, USA
- ⁸⁰State University of New York, Albany, New York 12222, USA
- ⁸¹University of Tennessee, Knoxville, Tennessee 37996, USA
- ⁸²University of Texas at Austin, Austin, Texas 78712, USA
- ⁸³University of Texas at Dallas, Richardson, Texas 75083, USA
- ⁸⁴INFN Sezione di Torino, I-10125 Torino, Italy
- ⁸⁵Dipartimento di Fisica Sperimentale, Università di Torino, I-10125 Torino, Italy
- ⁸⁶INFN Sezione di Trieste, I-34127 Trieste, Italy
- ⁸⁷Dipartimento di Fisica, Università di Trieste, I-34127 Trieste, Italy
- ⁸⁸IFIC, Universitat de Valencia-CSIC, E-46071 Valencia, Spain
- ⁸⁹University of Victoria, Victoria, British Columbia, Canada V8W 3P6
- ⁹⁰Department of Physics, University of Warwick, Coventry CV4 7AL, United Kingdom
- ⁹¹University of Wisconsin, Madison, Wisconsin 53706, USA

(Received 15 July 2008; published 9 September 2008)

Using 214 fb⁻¹ of data recorded by the *BABAR* detector at the PEP-II electron-positron collider, we study the decay $D_s^+ \rightarrow K^+ K^- e^+ \nu_e$. Except for a small S-wave contribution, the events with $K^+ K^-$ masses in the range 1.01–1.03 GeV/ c^2 correspond to ϕ mesons. For $D_s^+ \rightarrow \phi e^+ \nu_e$ decays, we measure the relative normalization of the Lorentz invariant form factors at $q^2 = 0$, $r_V = V(0)/A_1(0) = 1.849 \pm 0.060 \pm 0.095$, $r_2 = A_2(0)/A_1(0) = 0.763 \pm 0.071 \pm 0.065$ and the pole mass of the axial-vector form factors $m_A = (2.28_{-0.18}^{+0.23} \pm 0.18)$ GeV/ c^2 . Within the same $K^+ K^-$ mass range, we also measure the relative branching fraction $\mathcal{B}(D_s^+ \rightarrow K^+ K^- e^+ \nu_e)/\mathcal{B}(D_s^+ \rightarrow K^+ K^- \pi^+) = 0.558 \pm 0.007 \pm 0.016$, from which we obtain the total branching fraction $\mathcal{B}(D_s^+ \rightarrow \phi e^+ \nu_e) = (2.61 \pm 0.03 \pm 0.08 \pm 0.15) \times 10^{-2}$. By comparing this value with the predicted decay rate, we extract $A_1(0) = 0.607 \pm 0.011 \pm 0.019 \pm 0.018$. The stated uncertainties are statistical, systematic, and from external inputs.

DOI: 10.1103/PhysRevD.78.051101

PACS numbers: 12.15.Hh, 12.38.Gc, 13.20.Fc, 14.40.Lb

Charm semileptonic decays can help to validate predictions from lattice QCD through precise measurements of hadronic form factors. Such measurements have been performed by *BABAR* for the $D^0 \rightarrow K^- e^+ \nu_e$ decays [1]. The $D_s^+ \rightarrow \phi e^+ \nu_e$ [2] channel is well suited to study form factors in semileptonic decays of charm mesons to a vector particle because the ϕ meson is a narrow resonance which can be well isolated experimentally. Because of the higher mass of the spectator s -quark, form factor determinations for this process by lattice QCD are expected to be more accurate than for nonstrange D mesons. However, measurements of this decay mode are impacted by the lower production rate for D_s^+ mesons and higher backgrounds. Form factors in $D_s^+ \rightarrow \phi e^+ \nu_e$ have been previously studied by photoproduction experiments, at Fermilab [3–6], and by CLEOII at the CESR $e^+ e^-$ collider also operating at the $Y(4S)$ [7]. In charm meson semileptonic decays, a ϕ meson is expected to originate only from the D_s^+ . A possible contribution from the Cabibbo suppressed $D^+ \rightarrow \phi e^+ \nu_e$ decay, through the $d\bar{d}$ component of the ϕ meson [8] is neglected [9].

Using 214 fb⁻¹ of data collected at the $Y(4S)$ resonance by the *BABAR* detector, we measure the $D_s^+ \rightarrow K^+ K^- e^+ \nu_e$ channel decay characteristics, for events produced in the continuum $e^+ e^- \rightarrow c\bar{c}$. The analysis focuses on the $\phi e^+ \nu_e$ final state in the $K^+ K^-$ invariant mass range between 1.01 and 1.03 GeV/ c^2 . The ϕ resonance is dominant in this $K^+ K^-$ invariant mass region although a small S-wave component is observed, for the first time, through its interference with the ϕ .

The differential decay rate for $D_s^+ \rightarrow K^+ K^- e^+ \nu_e$ depends on five variables [10]: m_{KK}^2 , the mass squared of the

$K^+ K^-$ system; q^2 , the mass squared of the $e^+ \nu_e$ system; $\cos\theta_e$ ($\cos\theta_K$), where θ_e (θ_K) is the angle between the momentum of the e^+ (K^+) in the $e^+ \nu_e$ ($K^+ K^-$) rest frame and the momentum of the $e^+ \nu_e$ ($K^+ K^-$) system in the D_s^+ rest frame; and χ , the angle between the normals to the planes defined in the D_s^+ rest frame by the $K^+ K^-$ pair and the $e^+ \nu_e$ pair. When analyzing a D_s^- candidate, the direction of the K^- is used in place of the K^+ and χ is changed to $-\chi$. The expression for the differential decay rate as a function of these variables is given in Ref. [11]. Neglecting contributions proportional to the square of the electron mass, it depends on three hadronic form factors which are related to the three possible helicity values of the hadronic current. Restricting to S- and P-wave contributions, these form factors can be written as

$$\mathcal{F}_1 = \mathcal{F}_{10} + \mathcal{F}_{11} \cos\theta_K, \quad \mathcal{F}_2 = \frac{1}{\sqrt{2}} \mathcal{F}_{21}, \quad \mathcal{F}_3 = \frac{1}{\sqrt{2}} \mathcal{F}_{31}. \quad (1)$$

The form factors \mathcal{F}_{ij} depend only on m_{KK}^2 and q^2 ; \mathcal{F}_{10} characterizes the S-wave contribution, whereas the \mathcal{F}_{i1} correspond to the ϕ meson:

$$\mathcal{F}_{i1} = \sqrt{3\pi} q H_i(q^2, m) \mathcal{A}_\phi(m), \quad (2)$$

where the ϕ meson decay amplitude $\mathcal{A}_\phi(m)$ is taken to be a relativistic Breit-Wigner distribution with a mass-dependent width including a Blatt-Weisskopf damping factor [12]. The form factors $H_{1,2,3}$ can be expressed in terms of the Lorentz invariant form factors V and $A_{1,2}$ [13], for which we assume a q^2 dependence dominated by a single pole:

$$V(q^2) = \frac{V(0)}{1 - q^2/m_V^2}; \quad A_{1,2}(q^2) = \frac{A_{1,2}(0)}{1 - q^2/m_A^2}. \quad (3)$$

m_A and m_V are the pole masses, usually fixed to the values of corresponding resonance masses: $m_A = 2.5$ GeV/ c^2 ($\approx m_{D_{s1}}$) and $m_V = 2.1$ GeV/ c^2 ($\approx m_{D_s^*}$). At $q^2 = 0$, the ratios of the form factors V and A_2 relative to A_1 are denoted by r_V and r_2 , respectively. The S-wave contribution is parameterized assuming f_0 production:

*Deceased.

+Now at Temple University, Philadelphia, Pennsylvania 19122, USA.

‡Now at Tel Aviv University, Tel Aviv, 69978, Israel.

§Also with Università di Perugia, Dipartimento di Fisica, Perugia, Italy.

||Also with Università di Roma La Sapienza, I-00185 Roma, Italy.

¶Now at University of South Alabama, Mobile, Alabama 36688, USA.

**Also with Università di Sassari, Sassari, Italy.

$$\mathcal{F}_{10} = r_0 \frac{p_{KK} m_{D_s}}{1 - (q^2/m_A^2)} \frac{m_{f_0} g_\pi}{m_{f_0}^2 - m^2 - im_{f_0} \Gamma_{f_0}^0}, \quad (4)$$

where r_0 is a normalization factor and p_{KK} is the magnitude of the three-momentum of the K^+K^- system in the D_s^+ rest frame. The values of the f_0 parameters ($m_{f_0}, g_\pi, \Gamma_{f_0}^0$) are taken from Ref. [14].

A detailed description of the detector and the algorithms used for charged and neutral particle reconstruction and identification is provided elsewhere [15]. Monte Carlo (MC) samples of $Y(4S)$ decays, charm and other light quarks pairs from continuum events are generated using a GEANT4 [16]. Quark fragmentation, in continuum events, is described using the JETSET package [17]. Signal MC events are generated with 7 times the equivalent statistics of the data, using a simple pole model for the form factors with $m_A = 2.5 \text{ GeV}/c^2$ and $m_V = 2.1 \text{ GeV}/c^2$. The simulation of the characteristics of D_s^+ production is corrected to account for measured differences compared to data. Radiative processes are simulated with PHOTOS [18].

We reconstruct $D_s^+ \rightarrow K^+K^-e^+\nu_e$ decays, for D_s^+ produced in $e^+e^- \rightarrow c\bar{c}$ events. The hadronization of the $c\bar{c}$ system leads to the formation of two jets, emitted back-to-back in the center-of-mass (c.m.) frame. The analysis method is similar to the one used for the decay $D^0 \rightarrow K^-e^+\nu_e$ [1]. The only differences are that the cascade from a D^* is not used to evaluate the signal, and the detector performance for the D_s^+ reconstruction is measured using $D_s^+ \rightarrow \phi\pi^+$ decays rather than the cascade decay $D^{*+} \rightarrow D^0\pi^+, D^0 \rightarrow K^-\pi^+$.

The event thrust axis is determined from all charged and neutral particles in the c.m. system and its direction is required to be in the range $|\cos(\theta_{\text{thrust}})| < 0.6$ to minimize the loss of particles in regions close to the beam axis. A plane perpendicular to the thrust axis is used to define two hemispheres, equivalent to the two jets produced by quark fragmentation. In each hemisphere, we search for the decay products of the D_s^+ , namely, a positron, of momentum greater than $0.5 \text{ GeV}/c$, and two oppositely charged kaons. Since the ν_e momentum is unmeasured, a kinematic fit is performed, constraining the invariant mass of the candidate $K^+K^-e^+\nu_e$ system to the D_s^+ mass. In this fit, the D_s^+ direction and the neutrino energy are estimated from the other, charged and neutral, particles measured in the event. The D_s^+ direction is taken as the direction opposite to the sum of the momenta of all reconstructed particles, except for the kaons and the positron associated with the signal candidate. The neutrino energy is estimated as the difference between the total energy of the jet containing the candidate and the sum of the energies of all reconstructed particles in that hemisphere. The D_s^+ candidate is retained if the χ^2 probability of the kinematic fit exceeds 10^{-2} .

Sizable backgrounds arise from $Y(4S) \rightarrow B\bar{B}$ decays and two-jet events from $e^+e^- \rightarrow q\bar{q}$, $q = u, d, s, c$. Backgrounds are predominantly rejected by using two

Fisher discriminant variables that exploit differences in the production characteristics of hadrons in signal and background. The first variable is used to separate signal in jetlike $c\bar{c}$ events from $B\bar{B}$ with a more spherical topology. The chosen cut retains 71% of the signal and rejects 86% of the $B\bar{B}$ background. The second Fisher discriminant uses variables related to the different production characteristics of particles from D_s decays and c -quark fragmentation. The selected cut retains 71% of the signal decays, and rejects 72% of the background.

The overall signal efficiency is approximately 4.5%. Figure 1(a) shows the K^+K^- invariant mass distribution for the selected decays compared to the simulation. There are 31 839 events in the signal region, with an estimated background of 20.3%. About 70% of the total background is peaking, corresponding to a ϕ decay combined with an electron from another source. The interference between S- and P-waves generates an asymmetry in the $\cos\theta_K$ distribution which is revealed in Fig. 1(b), where events have been weighted by $\cos\theta_K$.

To extract N_S (the number of reconstructed signal events), r_V, r_2, m_A , and r_0 , we perform a binned maximum likelihood fit to the four-dimensional decay distribution in

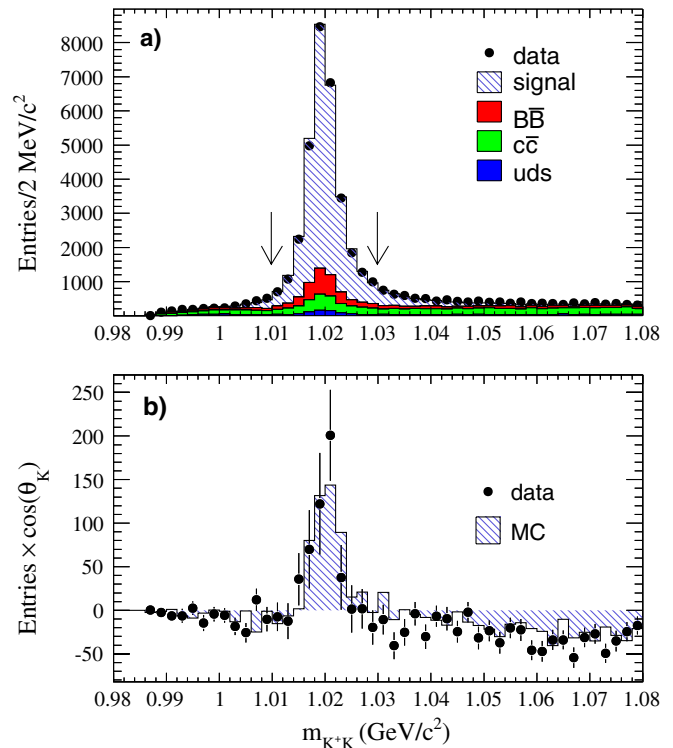


FIG. 1 (color online). (a) K^+K^- invariant mass distribution from data and simulated events. MC events have been normalized to the data luminosity according to the different cross sections. The arrows indicate the selected K^+K^- mass interval. In (b), each event is weighted by the measured value of $\cos\theta_K$. Negative entries are produced by the $c\bar{c}$ background asymmetry in $\cos\theta_K$.

the variables q^2 , $\cos\theta_e$, $\cos\theta_K$, and χ . The sensitivity to m_V is weak and we fix this parameter to 2.1 GeV/ c^2 . The data are divided into 625 bins, with five equal-sized bins per variable, and

$$\mathcal{L} = - \sum_{i=1}^{625} \ln \mathcal{P}(n_i^{\text{data}} | n_i^{\text{MC}}). \quad (5)$$

For each bin i , $\mathcal{P}(n_i^{\text{data}} | n_i^{\text{MC}})$ is the Poisson probability to observe n_i^{data} events when n_i^{MC} events are expected,

$$n_i^{\text{MC}}(\vec{\lambda}) = N_S \frac{\sum_{j=1}^{n_i^{\text{SMC}}} w_j(\vec{\lambda})}{W_{\text{tot}}(\vec{\lambda})} + n_i^{\text{BMC}}. \quad (6)$$

Here n_i^{SMC} is the number of signal MC events with reconstructed values of the four variables corresponding to bin i and n_i^{BMC} is the number of estimated background events. They are obtained from MC simulation, corrected for measured differences between data and simulation. Weights, w_j , are evaluated for each event, using the generated values of the kinematic variables, thus accounting for resolution effects. $W_{\text{tot}}(\vec{\lambda}) = \sum_{j=1}^{N^{\text{SMC}}} w_j(\vec{\lambda})$ is the sum of the weights for all simulated signal events (N^{SMC}) and $\vec{\lambda}$ corresponds to the parameters to be fitted. The data and results of the fit are shown in Fig. 2 and listed in Table I. From the fit we extract a contribution due to S-P wave

interference. The value obtained for r_0 corresponds to a S-wave fraction of $(0.22_{-0.08}^{+0.12})\%$ of the decay rate.

In the fitting procedure, two sources of statistical fluctuations are not included. They originate from the finite sample of simulated signal events and the estimate of the average number of background events in each bin. These effects are evaluated with parameterized simulations and included in the systematic uncertainties. Other systematic effects have been assessed to account for the uncertainties in the c -quark hadronization, the background contributions, and the remaining uncertainties in the simulation of the detector response. They are summarized in Table I.

Corrections to the simulation of the c -quark fragmentation were performed iteratively, comparing variables used in the event selection for samples of $D_s^+ \rightarrow \phi \pi^+$ decays and applying a weight which depends on the values of these variables. We adopt the observed changes in the fit parameters for the last step in this iterative process as an estimate of the systematic uncertainty. Furthermore we assume a 30% uncertainty in the simulation of radiative effects.

The peaking and combinatorial background components from $e^+e^- \rightarrow c\bar{c}$ events have been studied separately. The peaking background contributions are studied by measuring inclusive ϕ production in events with a fully reconstructed D^{*+} or D_s^+ decay. The combinatorial background

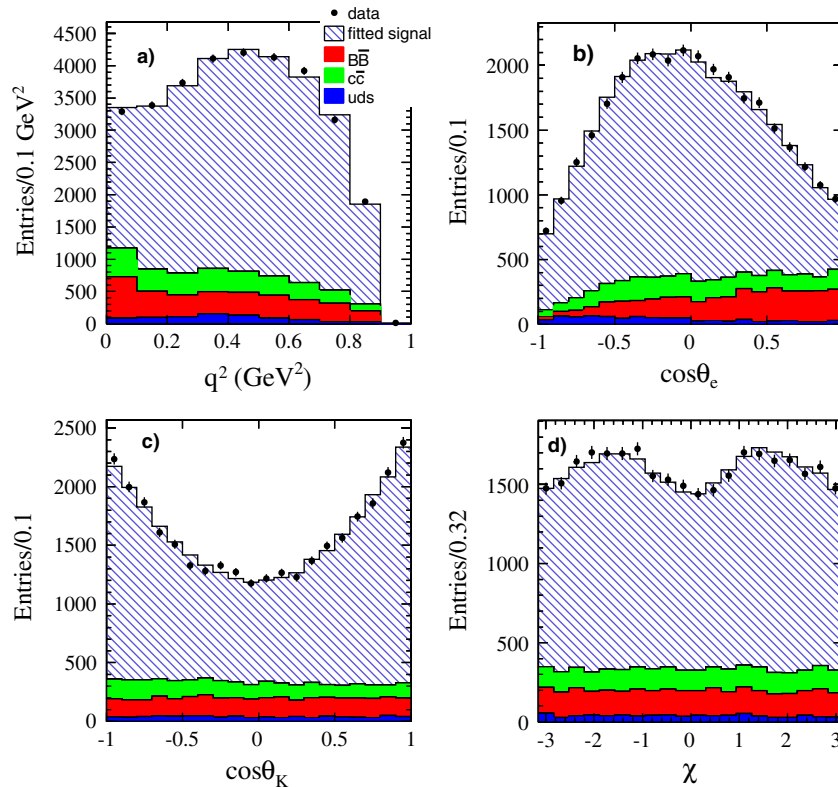


FIG. 2 (color online). Projected distributions of the reconstructed values of the four kinematic variables. The data (points with statistical uncertainties) are compared to the sum of four histograms, the fitted signal (light hatched) and the estimated background contributions (dark shaded).

TABLE I. Measured values of the parameters N_S , r_V , r_2 , m_A (GeV/c^2), r_0 (GeV^{-1}), their statistical and systematic uncertainties.

	N_S	r_V	r_2	m_A	r_0
Fitted value	25 341	1.849	0.763	2.28	15.1
Statistical uncertainty	178	0.060	0.071	+0.23 – 0.18	2.6
MC statistics	81	0.029	0.034	0.09	0.0
$c\bar{c}$ fragmentation	5	0.031	0.014	0.07	0.4
Background subtraction	480	0.081	0.049	0.14	0.6
Detector effects	12	0.021	0.021	0.07	0.6
Total syst. uncertainties	488	0.095	0.065	0.18	1.0

consists mainly of events with a charged lepton, one kaon from a D decay and a second kaon from fragmentation. We have measured the rate, momentum and angular distributions of K^\pm accompanying a D^0 , D^{*+} , or D_s^+ meson in data and corrected the corresponding simulation.

After these corrections, the K^+K^- distribution for selected signal events in MC and data agree to within 10% above $1.03 \text{ GeV}/c^2$, and this remaining difference is adopted as the uncertainty in the normalization of the combinatorial background. The $B\bar{B}$ background is obtained from the difference of the data recorded at the $Y(4S)$ resonance and the data recorded $40 \text{ MeV}/c$ below. The related systematic uncertainties are obtained from the statistical accuracy of these measurements and from the uncertainty (0.25%) between the relative normalization of the two data samples. Systematic uncertainties also originate from the simulation of the detector response. There are small differences in the efficiencies for charged particle reconstruction and electron and kaon identification. They lead to data-MC differences in the reconstruction of the D_s^+ direction and the neutrino energy. They are estimated using $D_s^+ \rightarrow \phi\pi^+$ decays.

We measure the $D_s^+ \rightarrow K^+K^-e^+\nu_e$ branching fraction relative to the decay, $D_s^+ \rightarrow K^+K^-\pi^+$ for which we adopt the K^+K^- mass interval, $1.0095\text{--}1.0295 \text{ GeV}/c^2$, to match the range used by CLEO-c for the $D_s^+ \rightarrow K^+K^-\pi^+$ branching fraction measurement [19]. Specifically, we compare the ratio of rates for the two channels in data and simulated events so that most systematic uncertainties cancel [1]. In the considered mass inter-

vals, we obtain $R_{D_s} = \frac{\mathcal{B}(D_s^+ \rightarrow K^+K^-e^+\nu_e)}{\mathcal{B}(D_s^+ \rightarrow K^+K^-\pi^+)} = 0.558 \pm 0.007 \pm 0.016$.

Systematic uncertainties are summarized in Table II. They originate mainly from selection criteria that are not common for the two channels. Differences in the impact of the two Fisher discriminants have been estimated by varying the selection cuts and differences in particle identification for electrons and pions are accounted for. The uncertainty on N_S is taken from the previous fit; it is dominated by uncertainties in the background evaluation.

We translate the ratio R_{D_s} to a branching fraction, using $\mathcal{B}(D_s^+ \rightarrow K^+K^-\pi^+) = (1.99 \pm 0.10 \pm 0.05)\%$ [19], correcting for the finite mass range used to select signal events ($86.37 \pm 1.22\%$), subtracting the S-wave contribution, and taking $\mathcal{B}(\phi \rightarrow K^+K^-) = (49.2 \pm 0.6)\%$ [8]. We find

$$\mathcal{B}(D_s^+ \rightarrow \phi e^+ \nu_e) = (2.61 \pm 0.03 \pm 0.08 \pm 0.15) \times 10^{-2},$$

where the last quoted uncertainty corresponds to external inputs.

In conclusion, we have studied the decay $D_s^+ \rightarrow K^+K^-e^+\nu_e$ with a sample of approximately 25 000 signal events, which greatly exceeds any previous measurement. This decay is dominated by the ϕ vector meson; we measure a small S-wave contribution, possibly associated with $f_0 \rightarrow K^+K^-$, corresponding to $(0.22_{-0.08}^{+0.12} \pm 0.03)\%$ of the $K^+K^-e^+\nu_e$ decay rate. We have extracted form factor parameters from a fit to the four-dimensional decay distribution, assuming single pole dominance and obtain: $r_V = V(0)/A_1(0) = 1.849 \pm 0.060 \pm 0.095$, $r_2 = A_2(0)/A_1(0) = 0.763 \pm 0.071 \pm 0.065$ and the pole mass of the axial-vector form factors $m_A = (2.28_{-0.18}^{+0.23} \pm 0.18) \text{ GeV}/c^2$. For comparison with previous measurements we also perform the fit to the data with fixed pole masses $m_A = 2.5 \text{ GeV}/c^2$ and $m_V = 2.1 \text{ GeV}/c^2$, ignoring also the small S-wave contribution.

The results on r_2 and r_V represent a large improvement in statistical and systematic precision compared to earlier measurements [3–7] (see Table III).

We also measure the relative branching fraction $\mathcal{B}(D_s^+ \rightarrow K^+K^-e^+\nu_e)/\mathcal{B}(D_s^+ \rightarrow K^+K^-\pi^+) = 0.558 \pm 0.007 \pm 0.016$, from which we obtain the total branching

TABLE II. Summary of the relative systematic uncertainties on R_{D_s} .

Source	Relative variation
Fisher variable against $c\bar{c}$ events	$\pm 1.77\%$
Fisher variable against $b\bar{b}$ events	$\pm 0.58\%$
Fitted signal (N_S)	$\pm 1.92\%$
PID corrections	$\pm 0.74\%$
D_s^+ production	$\pm 0.20\%$
Mass constrained fit	$\pm 0.61\%$
Total systematic uncertainty	$\pm 2.85\%$

B. AUBERT *et al.*PHYSICAL REVIEW D **78**, 051101(R) (2008)

TABLE III. Results from previous experiments and present measurements.

Experiment	r_V	r_2
E653 [3]	$2.3_{-0.9}^{+1.1} \pm 0.4$	$2.1_{-0.5}^{+0.6} \pm 0.2$
E687 [4]	$1.8 \pm 0.9 \pm 0.2$	$1.1 \pm 0.8 \pm 0.1$
E791 [5]	$2.27 \pm 0.35 \pm 0.22$	$1.57 \pm 0.25 \pm 0.19$
FOCUS [6]	$1.549 \pm 0.250 \pm 0.145$	$0.713 \pm 0.202 \pm 0.266$
CLEOII [7]	$0.9 \pm 0.6 \pm 0.3$	$1.4 \pm 0.5 \pm 0.3$
BABAR	$1.807 \pm 0.046 \pm 0.065$	$0.816 \pm 0.036 \pm 0.030$

fraction $\mathcal{B}(D_s^+ \rightarrow \phi e^+ \nu_e) = (2.61 \pm 0.03 \pm 0.08 \pm 0.15) \times 10^{-2}$. By comparing this quantity with the predicted decay rate, using the fitted parameters for the form factor pole ansatz we extract $A_1(0) = 0.607 \pm 0.011 \pm 0.019 \pm 0.018$. Here the third uncertainty refers to the combined value from external inputs, namely, the branching fractions of the D_s^+ into $K^+ K^- \pi^+$ and of the ϕ into $K^+ K^-$, the D_s^+ lifetime $[(500 \pm 7) \times 10^{-15} \text{ s}]$ and $V_{cs} = 0.9729 \pm 0.0003$. Predictions for this decay channel of lattice QCD calculations, in the quenched approximation [20], give: $r_V = 1.35_{-0.06}^{+0.08}$, $r_2 = 0.98 \pm 0.09$, $m_A = 2.42_{-0.16}^{+0.22} \text{ GeV}/c^2$,

and $A_1(0) = 0.63 \pm 0.02$. They agree with our determination of $A_1(0)$, r_2 , and m_A , but are lower than the measured value of r_V . The measured form factor's ratio r_2 is in agreement with the value obtained for the same parametrization for the vector decay $D \rightarrow \bar{K}^* e^+ \nu_e$, whereas r_V is 2 standard deviations higher [8]. The branching fraction presented here agrees well with the value $(2.68 \pm 0.13)\%$, consistent with the assumption of equal semileptonic decay widths for the different charm mesons.

We are grateful for the excellent luminosity and machine conditions provided by our PEP-2 colleagues, and for the substantial dedicated effort from the computing organizations that support BABAR. The collaborating institutions wish to thank SLAC for its support and kind hospitality. This work is supported by DOE and NSF (USA), NSERC (Canada), CEA and CNRS-IN2P3 (France), BMBF and DFG (Germany), INFN (Italy), FOM (The Netherlands), NFR (Norway), MES (Russia), MEC (Spain), and STFC (United Kingdom). Individuals have received support from the Marie Curie EIF (European Union) and the A. P. Sloan Foundation.

-
- [1] B. Aubert *et al.* (BABAR Collaboration), Phys. Rev. D **76**, 052005 (2007).
- [2] Charge conjugate states are implied throughout this article.
- [3] K. Kodama *et al.* (E653 Collaboration), Phys. Lett. B **309**, 483 (1993).
- [4] P.L. Frabetti *et al.* (E687 Collaboration), Phys. Lett. B **328**, 187 (1994).
- [5] E. M. Aitala *et al.* (E791 Collaboration), Phys. Lett. B **450**, 294 (1999).
- [6] J. M. Link *et al.* (FOCUS Collaboration), Phys. Lett. B **586**, 183 (2004).
- [7] P. Avery *et al.* (CLEO Collaboration), Phys. Lett. B **337**, 405 (1994).
- [8] W.-M. Yao *et al.* (Particle Data Group), J. Phys. G **33**, 1 (2006).
- [9] Using a singlet-octet mixing angle of 39° , the branching fraction $\mathcal{B}(D^+ \rightarrow \phi e^+ \nu_e) \sim 2 \times 10^{-6}$ and we expect less than 10 events from this source in our data sample.
- [10] N. Cabibbo and A. Maksymowicz, Phys. Rev. **137**, B438 (1965).
- [11] C.L. Y. Lee, M. Lu, and M.B. Wise, Phys. Rev. D **46**, 5040 (1992).
- [12] It is normalized such that: $\int_{m_\phi - \delta}^{m_\phi + \delta} (p^*/m) |\mathcal{A}_\phi(m)|^2 dm^2 \simeq 2 \arctan(2\delta/\Gamma_\phi^0)$ where δ is a small mass interval and Γ_ϕ^0 is the total width of the ϕ . The breakup momentum of the ϕ is denoted as p^* .
- [13] J. D. Richman and P. R. Burchat, Rev. Mod. Phys. **67**, 893 (1995).
- [14] M. Ablikim *et al.* (BES Collaboration), Phys. Lett. B **607**, 243 (2005).
- [15] B. Aubert *et al.* (BABAR Collaboration), Nucl. Instrum. Methods Phys. Res., Sect. A **479**, 1 (2002).
- [16] S. Agostinelli *et al.*, Nucl. Instrum. Methods Phys. Res., Sect. A **506**, 250 (2003).
- [17] T. Sjöstrand, Comput. Phys. Commun. **82**, 74 (1994).
- [18] E. Barberio and Z. Was, Comput. Phys. Commun. **79**, 291 (1994).
- [19] J. P. Alexander *et al.* (CLEO Collaboration), Phys. Rev. Lett. **100**, 091801 (2008).
- [20] J. Gill (UKQCD Collaboration), Nucl. Phys. B, Proc. Suppl. **106**, 391 (2002).